JOURNAL OF MATERIALS SCIENCE **33** (1998) 4905–4909

Probing of micromechanical properties of compliant polymeric materials

V. V. TSUKRUK*, Z. HUANG
College of Engineering and Applied Sciences, Western Michigan University, Kalamazoo, MI 49008-5062, USA
E-mail: vladimir@wmich.edu

S. A. CHIZHIK, V. V. GORBUNOV
Metal-Polymer Institute, National Academy of Science, Gomel, 246550, Belarus

Scanning force microscopy (SFM) was used for probing nanomechanical properties of compliant polymeric materials with lateral resolution from 20 to 140 nm and indentation depths from 2 to 200 nm. Sneddon's, Hertzian, and Johnson–Kendall–Roberts theories of elastic contacts were tested for a variety of polymeric materials with Young's modulus ranging from 1 MPa to 5 GPa. Results of these calculations were compared with a Sneddon's slope analysis widely used for hard materials. It was demonstrated that the Sneddon's slope analysis was ambiguous for polymeric materials. On the other hand, all models of elastic contact allowed probing depth profile of elastic properties with nanometre scale resolutions. The models gave consistent values of elastic moduli for indentation depth up to 200 nm with lateral resolution better 100 nm for most polymeric materials.

1. Introduction

Probing of local surface mechanical properties of various materials with a submicron resolution became a reality after the introduction of atomic force microscopy (AFM) and subsequent development in scanning force microscopy (SFM) technique [1–4]. However, to date, only a few attempts have been made to implement quantitative nanoprobing of mechanical properties of compliant polymers [4–9]. These attempts were based on classic mechanical approaches developed for "hard" metal and semiconductor surfaces [10–15]. The overall slope of force–distance curve and Sneddon's formula, were usually used for the treatment of SFM data [4–8, 10, 11]. However, this approach did not account for the specific features of compliant macromolecular materials such as very large indentation depth and viscoelastic behaviour. For quantitative nanoprobing of mechanical properties, the types of micromechanical deformation should be clarified and appropriate models of elastic contact for compliant polymer solids should be tested.

In the present communication, we report the results on micromechanical properties of polymeric materials based on classic theories of elastic contacts: Sneddon's, Hertzian, and Johnson–Kendall–Roberts (JKR) [10–15]. These theories were tested for indentation depths from 2 to 200 nm and for sample Young's modulus, E, from 1 MPa to 5 GPa and compared with a Sneddon's slope analysis.

* To whom correspondence should be addressed: fax 616-387-6517, email vladimir@wmich.edu.

2. Experimental procedure

The samples for investigation were selected to represent a variety of polymeric materials with a wide range of elastic properties. Polyisoprene rubber (Aldrich) had a nominal Young's modulus of 1–3 MPa [16]. Polyester-based Elastollan S60D53N and S69D53N polyurethanes (PUs) (BASF) and Dyreflex PT92004 PU (Bayer) had Young's moduli in the range of 10–40 MPa. Polyvynilchloride (PVC) was Selectophore from Fluka with Young's modulus in the range 1–4 GPa. Polystyrene (PS) with $M_w = 250\,000$ and $E = 2$–5 GPa was obtained from Janssen Chimica. Smooth polymer films of several micrometer thickness and several nanometre of surface microroughness were prepared by spin-coating technique (Headway spin-coater).

A combination of contact SFM mode in air and fluid (MilliQ water and absolute alcohol), and tapping and phase modes in air was used to characterize the polymer's surfaces according to the well established procedure on the Dimension 3000 microscope [17]. We used a set of V-shaped cantilevers with spring constants, k_n, of 0.25, 0.5, 0.58, 2.9 and 47 N m^{-1} to probe polymeric materials with very different elastic properties [18]. To estimate tip end radius, we scanned a reference sample of mixed gold nanoparticles tethered to a self-assembled monolayer [18].

3. Results and discussion

Typical force–distance curves used for calculation of elastic moduli are shown in Fig. 1 for rubber and Elastollan polyurethanes in water at 0.5 Hz approach–retract frequency. All curves obtained here are similar to

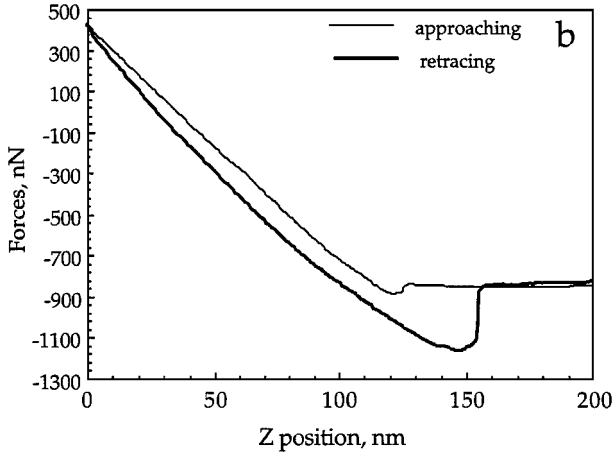

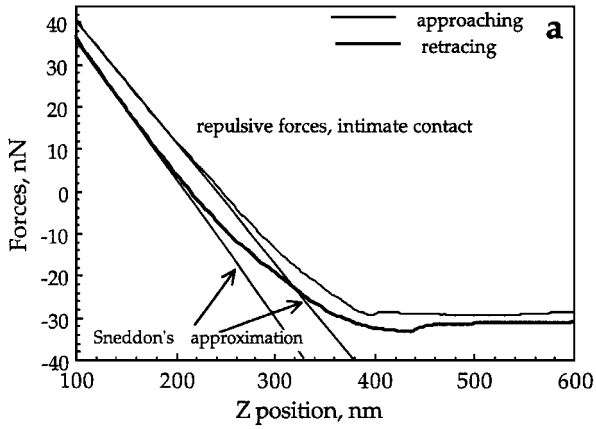

Figure 1 Force–distance data for the rubber sample (a) and for polyurethane (b) in approaching-retracing cycle, force scale in nN with arbitrary zero level, distance is in nm with arbitrary zero point. A thin line is the approaching part and a bold line is the retracing part. Linear approximation which can be used for Sneddon's analysis are shown by straight lines for rubber sample.

these ones and show jump-to-contact range, non-linear repulsive range in the approaching part, and pull-off range in the retracing part.

First, we tested a popular approximation frequently used for analysis of indentation data and calculation of Young's modulus from an overall slope of a force–distance curve by using the Sneddon's formula [5–8, 11–13]. The Sneddon's model gives the relationship between load gradient, $\mathrm{d}P/\mathrm{d}h$, and Young's modulus, E, in the form [13]

$$\frac{\mathrm{d}P}{\mathrm{d}h} = \frac{2A^{1/2}}{\pi^{1/2}}E \tag{1}$$

where $E = \{[(1-\nu_1^2)/E_1] + [(1-\nu_2^2)/E_2]\}^{-1}$, composite elastic modulus; E_1, E_2, ν_1, ν_2, Young's moduli and Poisson's ratio of a material and an indentor, respectively; P, normal load; A, contact area; and h, the indentation depth. By estimating $\mathrm{d}P/\mathrm{d}h$ and contact area for specific shape of the indentor (circular, pyramidic, and parabolic) one can evaluate elastic modulus from Equation 1. Fig. 1a shows examples of the standard slope analysis applied to the force–distance data for rubber sample. According to these estimations, $E = 3.6$ MPa for rubber, 40–135 MPa for PUs, 250 MPa for PVC and 3 GPa for PS. These values are reasonable

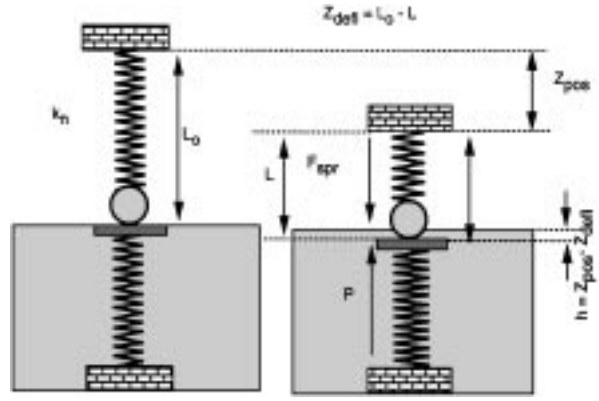

Figure 2 A double-spring model of elastic contact and major designations used in this work: left, unloaded state; right, loaded state.

for materials studied and can be used as a rough estimation of elastic moduli as can be discussed below.

To verify the applicability of different theories of elastic contact we used different approaches to analyse the repulsive force data from the contact point to the maximum indentation depth in the approaching mode for the rubber sample (Fig. 1a).

The equations for calculation of Young's modulus from cantilever deflection can be derived by using a two-spring linear model of interacting cantilever spring and elastic surface (Fig. 2) [7, 8]. Conditions for quasi-static equilibrium for this model are presented as equality of cantilever spring forces exerted and elastic surface response

$$k_n z_{defl} = P(h) \tag{2}$$

where $P(h)$ is normal load as a function of variable indentation depth $h = z_{pos} - z_{defl}$, z_{defl} is a measured vertical deflection of the SFM cantilever, z_{pos} is the vertical displacement of the SFM piezoelement (Fig. 2). By using relationships between normal load $P(h)$ and materials/indentation parameters offered in elastic contact models [10, 20, 21], one can obtain analytical expressions of Young's modulus for each model. For the polymer systems considered here, we assume $E_{tip} \gg E_{polymer}$ and, therefore, $E = E_{polymer}$ (elastic modulus of silicon tip is 160 GPa versus 0.01–1 GPa for polymers) [16].

After manipulation with initial Sneddon's equations for different models we receive

pyramidic indentor shape

$$E = \frac{(1-\upsilon^2)\pi^{1/2}}{2(2)^{1/2}\beta tg\alpha} k_n \frac{\Delta z_{defl,i,i-1}}{h\Delta h_{i,i-1}} \tag{3a}$$

parabolic indentor shape

$$E = \frac{(1-\upsilon^2)}{2(R)^{1/2}\beta} k_n \frac{\Delta z_{defl,i,i-1}}{h^{1/2}\Delta h_{i,i-1}} \tag{3b}$$

where $\beta = A_{cros}/A$, A_{cros} is cross-sectional indentor area at indentation depth h from the apex, β is equal to for elastic deformation [20]; α is half of pyramidic

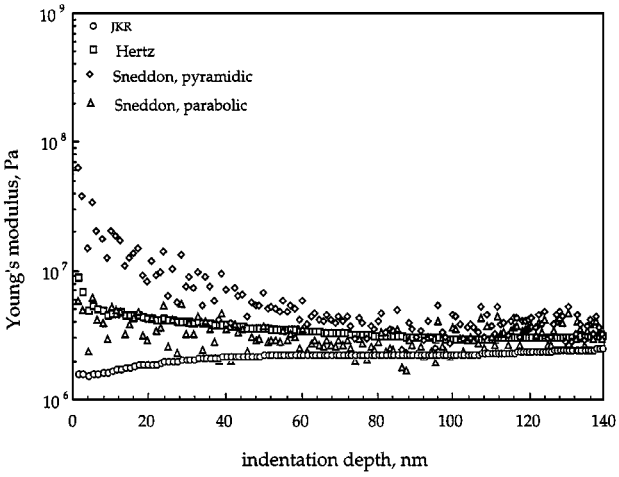

Figure 3 Comparison of different models for evaluation of depth dependence of elastic modulus (rubber sample).

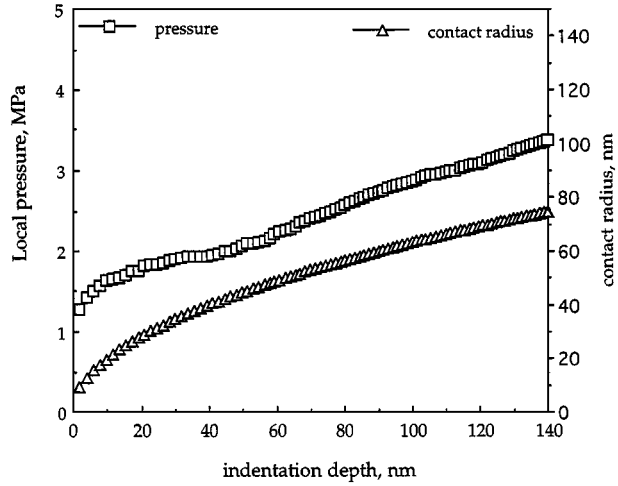

Figure 4 Variation of local contact pressure and the contact radius for rubber sample calculated for the Hertzian model.

angle of the indentor (35° for typical SFM pyramidic tip); R is tip radius; and i, $i-1$ refers to the adjacent indentor (tip) displacements.

Derivation of Young's modulus from the Hertzian model gives

$$E = \frac{3(1-v^2)}{4}\,\frac{k_n}{R^{1/2}}\,\frac{z_{defl}}{h^{3/2}} \tag{4}$$

with JKR model giving

$$E = \frac{9(1-v^2)}{4}\,Rk_n\Delta\left(\frac{P_1}{3Rh}\right)^{3/2} \tag{5}$$

where $P_1 = (3P_2 - 1)[9^{-1}(P_2+1)]^{1/3}$, $P_2 = (z_{defl}/\Delta + 1)^{1/2}$, and Δ is cantilever deflection at point where the tip loses contact with the surface [10–21].

To compare the results for various models, we used Sneddon's, Hertzian, and JKR approaches to process force–distance data and calculate Young's modulus at different penetration depth for rubber material (Fig. 3). Three immediate conclusions can be drawn from this data. First, at very low loads and small indentation depths less than 20 nm, unstable results are observed. Young's modulus variation in this range depends critically upon the selection of the initial contact point. We observed that variation of the initial point by ±2 nm can result in one order of magnitude variation of elastic modulus values at very small indentation depths. However, behaviour at larger indentation depth remains stable (for more discussions see Ref. 22). This phenomenon is known for the SFM cantilevers and is related to the destabilizing attractive force gradient in the vicinity of surfaces [15].

Second, Young's modulus for homogeneous polymers studied is independent of indentation depth and is virtually constant at the indentation depths larger than 20 nm (beyond surface instabilities). This behaviour is expected for homopolymers studied here. The maximum indentation depth for purely elastic deformation varies reciprocally to the elastic properties of materials from 200 nm for rubber to 20 nm for PS. Local contact pressure gradually increases with indentation depth as calculated using the Hertzian model and shown in Fig. 4 for rubber sample. The contact radius gradually increases with the normal load from up to 80 nm for rubber at maximum loads (Fig. 4). The contact radius at maximum loads decreases to 50–60 nm for PUs, and is only about 10 nm for hard PS.

Third, all three approaches give convergent results and very close absolute values of Young's modulus at indentation depths higher than 20 nm. Deviations of elastic modulus values obtained for the Sneddon's pyramidic model at very low indentation depth are related to the underestimation of the initial contact area. The Sneddon's parabolic model gives virtually identical results (with higher scattering) with the Hertzian model. On the other hand, the Hertzian model gives 25% higher absolute value of elastic modulus as compared to JKR calculations. This difference is caused by non inclusion of the zero load contact area in the Hertzian model [20–21].

Next, we considered the limitations of sphere–plane models related to elastic deformations larger than sphere radius. We calculated the indentation depth versus the normal load for Hertzian sphere–plane and cone–plane models (Fig. 5). As we concluded from the comparison with experimental data for rubber, the Hertzian model nicely describes experimental data at small indentation depths but deviates significantly for $h > 70$ nm. Deviation reaches 10% at $h = 150$ nm. On the other hand, for $h > 80$ nm, the cone–plane model describes experimental behaviour very closely (Fig. 5). Therefore, the sphere–plane model can be used in the range of indentation depth up to a diameter of the SFM tip ($h = 50$–100 nm) which is typical range of depths probed for elastomers. Larger indentation depths ($h > 2R$) should be considered with caution and corrections must be included if precision better than 10–20% is required.

The Hertzian model was used to calculate the depth profile of elastic moduli for a set of polymeric materials (Fig. 6). The experimental data is presented along with the bars representing range of Young's modulus measured for bulk materials. This plot shows the very close correlation between the level of elastic moduli

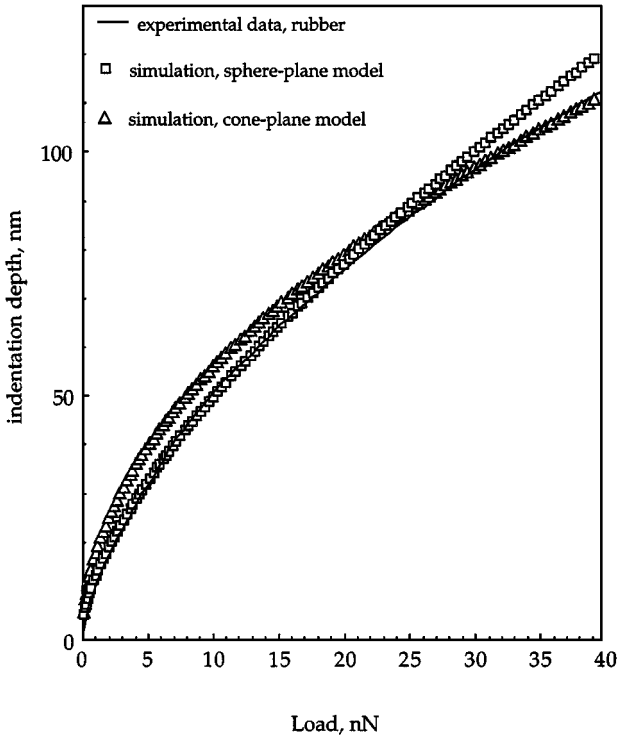

Figure 5 Variation of indentation depth versus load for sphere–plane (squares) and cone–plane (triangles) models in comparison with experimental data for rubber (solid line).

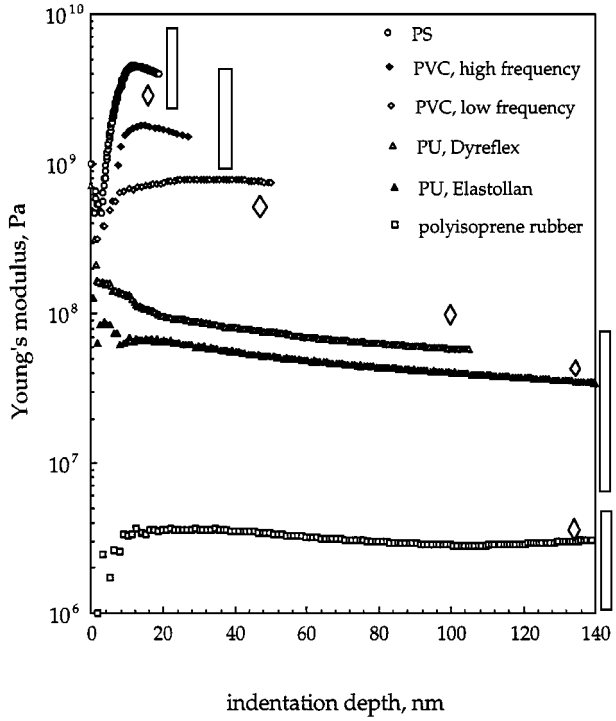

Figure 6 Summarized data for the depth variation of elastic modulus for rubber, two different PUs, PVC at high and low frequencies, and PS. Bars demonstrate the range of elastic bulk modulus variation for specific materials (frequency, molecular weight, composition dependent). Rhombic marks show the values of Young's moduli determined from the Sneddon's slope analysis.

probed by SFM and mechanical properties of bulk materials. The absolute values of elastic moduli vary by four orders of magnitude and ranging from 2 MPa for rubber to 5 GPa for PS. Absolute values determined from SFM measurements tend to be closer to the higher limit the Young's moduli determined from tensile experiments as is expected for compression testing [23]. All data are shown here at 0.5 Hz frequency of contact. Additional measurements at various frequencies demonstrate very strong frequency dependence for various polymeric materials as will be discussed in a separate publication. As an example, we display two very different elastic modulus curves for PVC obtained at high (90 Hz) and low (4.6 Hz) frequencies (Fig. 6).

Finally, we estimated the accuracy of a linear approximation for the Sneddon's model (Equation 1). Direct comparison of elastic moduli obtained from modulus–depth curves in Fig. 6 with the slope analysis presented in Fig. 1 shows significant differences in absolute values (see data for comparison in Fig. 6). Typical deviation of the slope analysis results from the complete calculations according to Equations 2–5 is about 30% but it can reach as much as 100% in the case of significant non-linearity of force–distance data and non-optimal cantilever stiffness (e.g. for PUs or PS).

4. Conclusions

By combining optimal cantilever parameters and experimental conditions we can obtain reliable force–distance data which is appropriate for further contact mechanics analysis for wide selection of polymeric materials with elastic moduli ranging from 1 MPa to several GPas. Both Sneddon's and Hertzian models of elastic contact give consistent and reliable results in the range of indentation depth from 2–20 to 30–200 nm for different materials with lower limit dictated by surface instabilities and maximum depth determined by elastic deformation limit. The Hertzian model of elastic contact gives reliable absolute values of elastic modulus at given experimental conditions that eliminate strong capillary forces. The deviation is estimated to be about 25% if compared with JKR model for very compliant materials, and is much smaller for harder polymers. Within this accuracy, the Hertzian model is applicable to a wide range of polymeric materials from rubbers to glassy polymers. However, obtaining higher precision requires the employment of more complicated JKR model and measurements of local interfacial energies. This work is in progress.

In spite of large elastic indentation depth for compliant polymeric materials and difficulties in judgment of cantilever selection criteria, simple slope analysis of force–distance data is very ambiguous and can be recommended only for crude estimation of elastic moduli with possible 30–100% error. Direct calculation of elastic moduli implemented here gives reliable results on depth modulation of elastic properties with vertical resolution better than 10 nm and lateral resolution in the range of 20–150 nm for different materials. Close correlation is observed between elastic moduli determined by SFM and known values for bulk materials. A large range of elastic polymer properties can be probed if a selection of cantilever stiffness from 0.1 to 50 $N\,m^{-1}$ is available. Elastic moduli can be measured as low as several MPas for rubbers to as high as several GPas for

glassy polymers. The SFM ability to probe depth profiles of elastic properties at the submicron scale is unparallelled for nanocomposite materials with spatially distributed mechanical response.

Acknowledgements

This work is supported by The Surface Engineering and Tribology Program, The National Science Foundation, CMS-94-09431 and CMS-9610408 Grants and Becton Dickinson Corp. Donation of polyurethane materials by BASF and Bayer is greatly appreciated. The authors thank J. Hazel for assistance and helpful discussion.

References

1. G. BINNIG, C. F. QUATE and C. GERBER, *Phys. Rev. Lett.* **12** (1986) 930.
2. D. SARID, "Scanning force microscopy" (Oxford University Press, New York, 1991).
3. B. RATNER and V. V. TSUKRUK, (eds) "Scanning probe microscopy of polymers" (ACS Symposium Series, Washington DC, v. 694, 1997).
4. V. V. TSUKRUK, *Rubber Chem. & Techn.* 1998 **10**, 430, 1997.
5. M. R. VANLANDINGHAM, S. H. MCKNIGHT, G. R. PALMESE, R. F. EDULJEE, J. W. GILLESPIE and R. J. MCCULOUGH, *J. Mater. Sci. Lett.* **16** (1997) 117.
6. M. R. VANLANDINGHAM, S. H. MCKNIGHT, G. R. PALMESE, J. R. ELLINGS, X. HUANG, T. A. BOGETTI, R. F. EDULJEE and J. W. GILLESPIE, *J. Adhesion* **31** (1997) 64.
7. M. RADMACHER, M. FRITZ, C. M. KACHER, J. P. CLEVELAND and P. K. HANSMA, *Biophys. J.* **70** (1996) 556.
8. N. J. TAO, S. M. LINDSAY and S. LEES, *ibid.* **63** (1992) 1165.
9. K. L. WAHL, S. V. STEPNOWSKI and W. L. UNERTL, *J. Tribology* in press (1998).
10. B. BHUSHAN, (ed.), "Micro/nanotribology and its applications" (NATO ASI Series E330, Kluwer Acad. Publ., Dordrecht, 1997).
11. S. M. HUES, R. J. COLTON, E. MEYER and H.-J. GUNTHERODT, *MRS Bull.* **18(1)** (1993) 41.
12. S. M. HUES, C. F. DRAPER and R. J. COLTON *J. Vac. Sci. Technol.* **B12** (1994) 2211.
13. I. N. SNEDDON, *Int. J. Engng. Sci.* **3** (1965) 47.
14. G. M. PHART, W. C. OLIVER and F. B. BROTZEN, *J. Mater. Res.* **7** (1992) 613.
15. N. A. BURNHAM, D. D. DOMINGUEZ, R. L. MOWERY and R. J. COLTON, *Phys. Rev. Lett.* **64** (1990) 1931.
16. J. J. AKLONIS and W. J. MACKNIGHT, "Introduction to polymer viscoelasticity" (J. Wiley & Sons: NY, 1983).
17. V. V. TSUKRUK and D. H. RENEKER, *Polymer* **36** (1995) 1791.
18. M. P. EVERSON, V. N. BLIZNYUK and V. V. TSUKRUK, *J. Tribology* **120**, 489, 1998.
19. V. N. BLIZNYUK, J. H. HAZEL, J. WU and V. V. TSUKRUK, in "Scanning probe Microscopy of polymers," edited by B. Ratner and V. V. Tsukruk (ACS Symposium Series, Washington DC, v. 690, 1997.)
20. A. I. SVIRIDENOK, S. A. CHIZHIK and M. I. PETROKOVETS, "Mechanics of a discreet friction contact" (Nauka I Tekhnika, Minsk, 1990).
21. K. L. JOHNSON, K. KENDALL and A. ROBERTS, *Proc. R. Soc., London* **A324** (1971) 301.
22. S. A. CHIZHIK, Z. HUANG, V. V. GORBUNOV, N. K. MYSHKIN and V. V. TSUKRUK, *Langmuir*, 14, 2606, 1998.
23. L. E. NIELSEN and R. F. LANDEL, "Mechanical properties of polymers and composites" (Marcel Dekker, NY, 1994).

Received 29 January
and accepted 2 July 1998